

Spin reorientation transition of Fe films in magnetically coupled Fe/Cu/Ni/Cu(001)H. J. Choi,¹ W. L. Ling,¹ A. Scholl,² J. H. Wolfe,¹ U. Bovensiepen,^{1,*} F. Toyama,¹ and Z. Q. Qiu¹¹*Physics Department, University of California Berkeley, Berkeley, California 94720*²*Advanced Light Source, Lawrence Berkeley National Laboratory, Berkeley, California 94720*

(Received 19 April 2002; published 26 June 2002)

Spin reorientation transition (SRT) of Fe film in the magnetically coupled Fe/Cu/Ni/Cu(001) system was investigated by surface magneto-optic Kerr effect and photoemission electron microscopy. We found that the Fe in-plane magnetic remanence within the SRT region oscillates with the Cu layer thickness with a periodicity exactly half of that of the magnetic interlayer coupling. Element specific domain imaging shows that the Fe stripe domains within the SRT region are washed away by the magnetic interlayer coupling in such a way that the majority domain size increases without changing the minority domain size. These results are discussed in terms of the virtual magnetic field produced by the magnetic interlayer coupling.

DOI: 10.1103/PhysRevB.66.014409

PACS number(s): 75.70.Ak, 75.30.Kz, 75.50.Bb, 75.70.Rf

Theoretically, magnetic long-range order does not exist in a two-dimensional (2D) isotropic Heisenberg system at any finite temperature,¹ but could be triggered by a uniaxial magnetic anisotropy.² Experimentally, this issue has been addressed by investigating the so-called spin reorientation transition (SRT) in magnetic thin films whose in-plane magnetic shape anisotropy can be balanced out by its perpendicular crystalline magnetic anisotropy. At the SRT point where the magnetization switches its direction from a perpendicular to an in-plane direction, the overall uniaxial magnetic anisotropy (magnetocrystalline and the shape anisotropies) approaches zero so that an isotropic 2D Heisenberg system is expected. Thus an investigation of the magnetic remanence at the SRT point should elucidate the origin of 2D magnetic long-range order. Pappas *et al.*³ studied the SRT in Fe/Cu(100) using spin polarized electron spectroscopy and observed that the magnetic remanence vanishes within a pseudogap at the SRT point. Applying the more precise surface magneto-optic Kerr effect (SMOKE) technique, Qiu *et al.*⁴ studied Fe/Ag(100) and found that the magnetization is not exactly zero but exhibits asymmetric behavior within the pseudogap. Meanwhile Allenspach and Bischof⁵ investigated Fe/Cu(100) using scanning electron microscopy with polarization analysis (SEMPA) and observed that the reduced magnetization in the pseudogap is associated with the formation of stripe domains. These experimental observations promoted the examination of possible new magnetic phases in the 2D Heisenberg system. Theoretically, Yafet and Gyorgy noticed that the stripe domain phase is energetically favored over a single domain phase at zero temperature, and that the domain size shrinks rapidly into the submicron range as the uniaxial magnetic anisotropy approaches zero.⁶ Kashuba *et al.* extended the work to nonzero temperatures and found that the stripe domain phase survives the thermal fluctuations.^{7,8} Following these two studies, many other theoretical efforts^{9–11} have been made to address the magnetic phase in the SRT region. It has been speculated that the formation of the stripe domains is a result of the competition between the short-range magnetic exchange interaction and the long-range magnetic dipolar interaction. An important consequence of this speculation is that the stripe-domain width reflects an intrinsic length scale that should remain

finite even within an external magnetic field.^{7,8} Thus it is of importance to investigate experimentally the stripe domain phase within a magnetic field in order to understand its physical nature.¹² Despite the great theoretical activities, there has been little experimental progress in the last few years, mainly due to the difficulty of obtaining domain images within a magnetic field. Stripe domains are usually imaged by electron microscope [SEMPA or photoemission electron microscopy (PEEM)] which can resolve a weak magnetic signal with high spatial resolution. Unfortunately it is difficult to operate an electron microscope within a magnetic field. Although much effort has been made in overcoming this difficulty, there has been a lack of direct stripe domain imaging within a magnetic field. In this paper, we report on the SRT in a magnetically coupled Fe/Cu/Ni/Cu(100) system. We show that the Fe-Ni interlayer coupling behaves as a *virtual magnetic field* so that information on the stripe domains within a magnetic field can be obtained by element specific domain imaging using PEEM in this magnetically coupled system.

A 10-mm-diameter Cu(001) single-crystal substrate was mechanically polished with 0.25- μm diamond past finish, and electropolished as previously reported.¹³ The sample of Fe/Cu/Ni [30 monolayers (ML)] was epitaxially grown on the Cu(001). To systematically vary the Fe and Cu thicknesses, the Fe and Cu were grown into wedges perpendicular to each other so that their thicknesses can be controlled independently (Fig. 1). The Ni and Cu layers were grown at room temperature, but the Fe film was grown at ~ 150 K to ensure the existence of the SRT.⁵ The sample for PEEM measurement was magnetized in a 1-kOe magnetic field perpendicular to the film surface, prior to the Fe film growth, to wipe out the Ni magnetic domains, ensuring a uniform exchange coupling field of Ni on Fe. After the Fe film growth, the sample was capped with a 30-ML Cu protective layer and transferred into the PEEM chamber at beamline 7.3.1.1 of the Advanced Light Source (ALS) at Lawrence Berkeley National Laboratory (LBNL). The magnetic domain images were obtained by taking the ratio of L_3 and L_2 edges¹⁴ utilizing the effect of magnetic circular dichroism (XMCD). For SMOKE measurement, two pairs of electromagnets were used to apply magnetic field either perpendicular or parallel

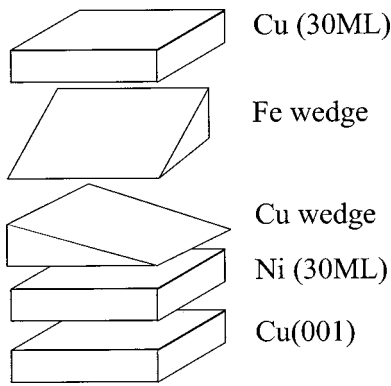


FIG. 1. Schematic drawing of the double wedge sample that allows the independent control of the Fe and Cu thicknesses.

to the film plane so that polar and longitudinal hysteresis loops can be obtained without the need of moving the sample.

SMOKE measurements on 30 ML of Ni/Cu(001) show only polar hysteresis loops with full remanence, confirming that the 30-ML Ni layer has a perpendicular magnetization.¹⁵ To determine the Fe-Ni interlayer coupling, we performed polar SMOKE measurements along the Cu wedge at 4.7 ML of Fe whose magnetization is perpendicular to the film plane. Typical hysteresis loops for antiferromagnetic coupling (AFC) and ferromagnetic coupling (FC) are shown in Fig. 2. For the FC case, a square loop with full remanence is obtained because the Ni and Fe magnetizations are coupled to the same direction. For the AFC case, the Ni and Fe magnetizations are antiparallel at low magnetic field so that the total magnetization is reduced (the nonzero remanence is due to the unbalanced SMOKE signals from the Ni and Fe films). At high magnetic field, the Zeeman energy overcomes the AFC to align the Ni and Fe magnetizations to the same direction. Therefore the saturation field (H_s) in the AFC hys-

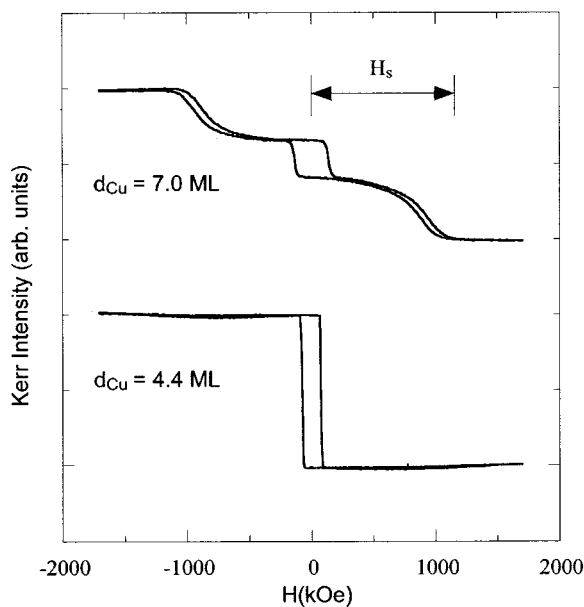


FIG. 2. Typical AFC (top) and FC (bottom) hysteresis loops of Fe(4.7 ML)/Cu/Ni(30 ML)/Cu(001) sample.

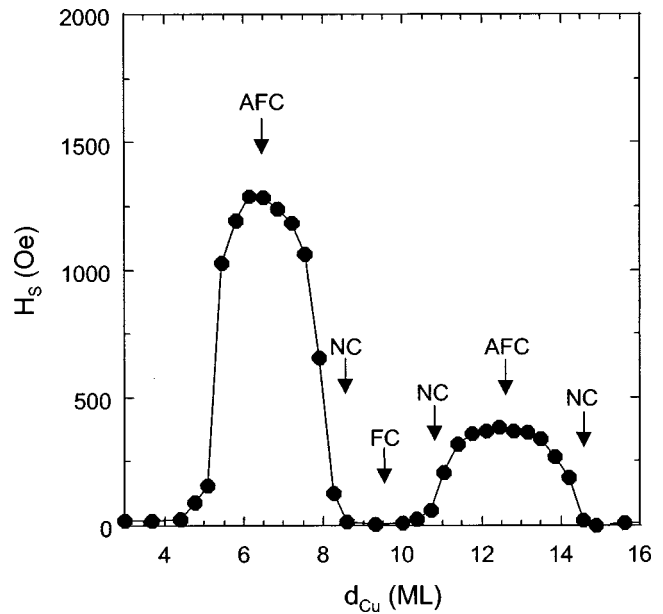


FIG. 3. Saturation field (H_s) versus Cu thickness (d_{Cu}) from Fe(4.7 ML)/Cu/Ni(30 ML)/Cu(001) sample. Arrows show the locations of AFC, FC, and NC, respectively.

teresis loop is proportional to the AFC strength. Figure 3 shows the saturation field (H_s) as a function of the Cu thickness (d_{Cu}). The oscillations of the H_s versus d_{Cu} represent the oscillatory interlayer coupling between the Fe and Ni films across the Cu spacer layer. Because of the dislocation-induced surface roughness in Ni/Cu(001),¹⁶ only long-period (5.8-ML) oscillations were observed, which is consistent with a previous result.¹⁷

To study the SRT, SMOKE measurements were performed as a function of the Fe film thickness (d_{Fe}) at $d_{Cu} = 7.0, 8.6,$ and 9.6 ML which correspond to the AFC, no-coupling (NC), and FC, respectively. As a reference, SMOKE measurements were also taken at a very thick Cu thickness (>30 ML) to generate the results of the Fe/Cu(001) system. Because of the perpendicular magnetization of the 30 ML of Ni, we can only single out the in-plane component of the Fe magnetization by performing longitudinal SMOKE measurements. The in-plane magnetic remanence ($M_{R,\parallel}$) of the Fe film develops from zero after a critical thickness and saturates quickly with increasing Fe thickness (Fig. 4). This is the typical SRT behavior with the developing region referred previously to the SRT pseudogap⁴ within which the stripe domains were observed.⁵ First, we observed that the onset of $M_{R,\parallel}$ occurs at the same Fe thickness, indicating that the Fe-Ni interlayer coupling has little effect on the SRT thickness. Second, we found that the $M_{R,\parallel}$ within the pseudogap depends sensitively on the interlayer coupling— $M_{R,\parallel}$ behaves exactly the same as in Fe/Cu(001) for the NC case and is reduced for both the AFC and FC cases. It should be pointed out that the SMOKE laser beam covers ~ 0.25 -ML Fe thickness due to the wedge shape, thus each point in Fig. 4 should represent an averaged result over the ~ 0.25 -ML thickness range. To ensure that the results of Fig. 4 are associated with the SRT, we measured $M_{R,\parallel}$ as a function of Cu thickness at $d_{Fe} = 5.7$ and 6.4 ML which are

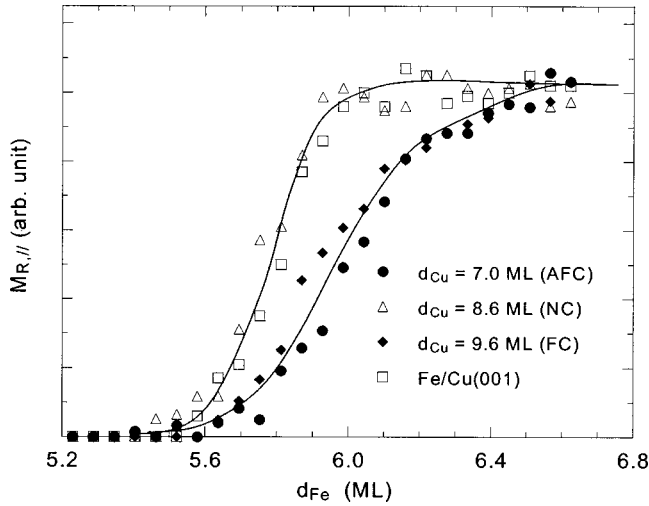


FIG. 4. In-plane magnetic remanence ($M_{R,||}$) obtained from longitudinal SMOKE measurements versus Fe film thickness (d_{Fe}) in the spin reorientation transition region. The solid lines are guides to the eye.

inside and outside of the SRT pseudogap, respectively (Fig. 5). For $d_{Fe} = 5.7$ ML $M_{R,||}$ clearly oscillates with Cu thickness. Moreover, the oscillation periodicity equals half of that in the magnetic interlayer coupling with the maxima and minima occurring at NC and AFC/FC, respectively. For $d_{Fe} = 6.2$ ML the oscillations of $M_{R,||}$ disappear [Fig. 5(b)], supporting our assertion that the oscillations of the $M_{R,||}$ are associated with the SRT.

To understand the above results, recall that the magnetic interlayer coupling can be expressed with the Ni and Fe magnetization vectors (\vec{M}_{Ni} and \vec{M}_{Fe}) as $E = -J\vec{M}_{Fe} \cdot \vec{M}_{Ni}$, where J oscillates with d_{Cu} . If the Ni layer forms magnetic single domain, i.e., \vec{M}_{Ni} varies very little in space, the coupling can be approximated by $E = -\vec{M}_{Fe} \cdot \vec{H}$ with \vec{H}

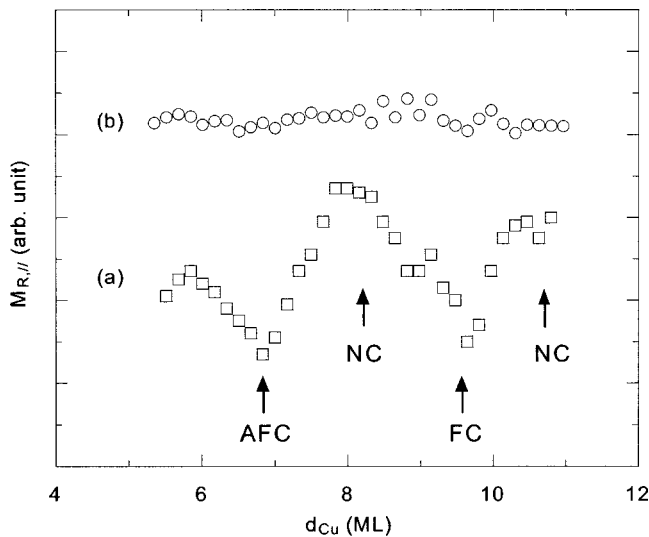


FIG. 5. In-plane magnetic remanence ($M_{R,||}$) of Fe film versus Cu thickness for (a) $d_{Fe} = 5.7$ ML and (b) $d_{Fe} = 6.4$ ML which are within and outside the SRT pseudogap, respectively.

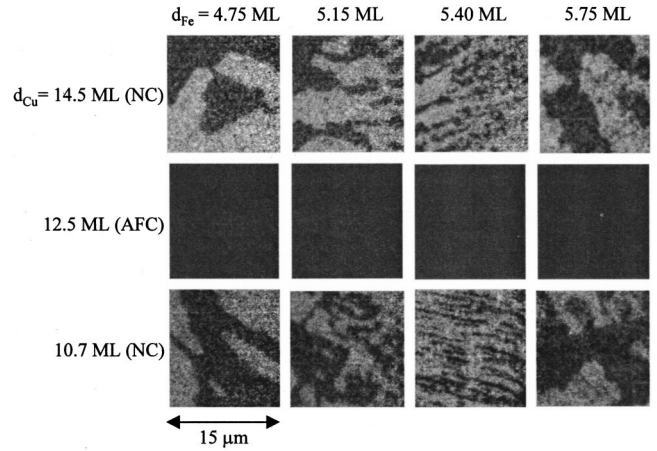


FIG. 6. PEEM images of Fe film magnetic domains with Fe film thickness at $d_{Cu} = 10.7, 12.5,$ and 14.5 ML which correspond to NC, AFC, and NC, respectively. Stripe domains are present for $d_{Fe} = 5.4$ ML at NC positions.

$= J\langle \vec{M}_{Ni} \rangle$. This formula suggests that the magnetic behavior of the Fe film in a coupled system represents the behavior of a single Fe film within a virtual magnetic field $\vec{H} = J\langle \vec{M}_{Ni} \rangle$. Under this equivalence, Fig. 3 reveals the in-plane magnetization of a single Fe film within a perpendicular magnetic field $\vec{H} = J\langle \vec{M}_{Ni} \rangle$. Within the SRT pseudogap, a perpendicular magnetic field tends to wipe out the stripe domains to saturate the magnetization in the perpendicular direction,¹² hence reducing the in-plane magnetization. That is why the minima of $M_{R,||}$ in Fig. 5(a) occur exactly at the peaks of AFC and FC where the virtual perpendicular magnetic field reaches its maximum. This also explains why the oscillation periodicity in Fig. 5(a) is half of that in the magnetic interlayer coupling because the response of the in-plane magnetization is independent to the direction of a perpendicular magnetic field. Moreover, it also becomes clear why the $M_{R,||}$ in Fig. 4 for NC (noncoupling) behaves in the same way as in Fe/Cu(001) because NC gives a zero virtual magnetic field.

To obtain the microscopic behavior of the Fe stripe domains within a perpendicular magnetic field, we did element-specific domain imaging in the magnetically coupled Fe/Cu/Ni(30-ML)/Cu(100) system. Ni PEEM images confirm that the Ni layer has a single domain structure, thus we only show the Fe domain images in this paper. We first studied Fe magnetic domains as a function of the Fe film thickness with different Fe-Ni interlayer coupling. Figure 6 shows three representative series of Fe domain images at $d_{Cu} = 10.7, 12.5,$ and 14.5 ML, which correspond to NC, AFC, and NC, respectively. Away from the SRT region, we observed only the single magnetic domain of the Fe film. Near the SRT, however, the Fe film exhibits characteristic domain evolution. At the NC Cu thickness, the Fe film first breaks into big sized magnetic domains and then evolves into stripe domains at the SRT point. The stripe domains are submicron sized and have a preferred direction, in agreement with previous observations on the Fe/Cu(001) system.⁵ At the AFC peak position, there exists only single domain throughout the Fe thick-

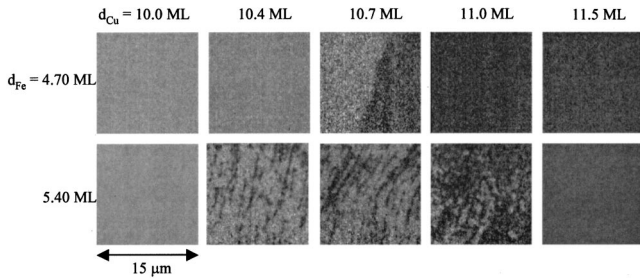


FIG. 7. PEEM images of Fe film magnetic domains for $d_{\text{Fe}} = 4.7$ and 5.4 ML as a function of Cu thickness around the NC boundary of $d_{\text{Cu}} = 10.7$ ML.

ness range. This is also true at other AFC and FC peak positions. The absence of the magnetic domains at the AFC and FC peak positions shows that the virtual magnetic field at these positions is strong enough to wipe out the Fe domains.

We then investigated the Fe magnetic domains as a function of the Cu thickness at the SRT point ($d_{\text{Fe}} = 5.4$ ML). This study provides information of the stripe domains within a perpendicular magnetic field. For comparison, we also took domain images at a lower Fe thickness of ($d_{\text{Fe}} = 4.75$ ML) to visualize the Ni-Fe interlayer coupling. Figure 7 shows representative Fe domain images in the evolution from FC to AFC ($10 < d_{\text{Cu}} < 12$ ML). For $d_{\text{Fe}} = 4.7$ ML, a single domain state is observed except at the NC position where a sharp boundary divides up (white) and down (dark) magnetization areas corresponding to the FC and AFC regions. For $d_{\text{Fe}} = 5.4$ ML, stripe domains with equal areas of up and down regions are present at the NC point. Moving away from the NC point, towards either the FC or AFC region, the stripe domains are gradually swept away by the virtual magnetic field. It is important to note that the stripe domains evolve in such a way that the average size of the majority domains grows while that of the minority domains remains unchanged, i.e., the magnetization increases by reducing the minority domain density but not its width. This property distinguishes the stripe domains from ordinary magnetic domains in which a magnetic field not only increases the majority domain size but also reduces the minority domain size.

The characteristic property of the stripe domains that the minority domain width remains finite within a perpendicular magnetic field was predicted by theory a while ago.⁷ When considering stripe domains of width L within a perpendicular magnetic field H , Kashuba and Pokrovsky found that the magnetic field breaks the up-down symmetry to change the majority and minority domain widths into $L + \delta$ and $L - \delta$, respectively. Due to the dipolar interaction, however, the L and δ diverge in a similar manner of $L \sim 1/\sqrt{1 - (H/H_S)^2}$ and $\delta \sim 2 \sin^{-1}(H/H_S)/\pi\sqrt{1 - (H/H_S)^2}$, where H_S is the saturation field. This property leaves the minority domain width $L - \delta$ finite as the magnetic field wipes out the stripe domains.⁷ To have a quantitative understanding, we constructed histogram of the minority domain width at five different Cu thicknesses. Each histogram consists of ~ 1000 measurements from the PEEM image (Fig. 8). The perpendicular magnetization (M_{\perp}) was also calculated by taking

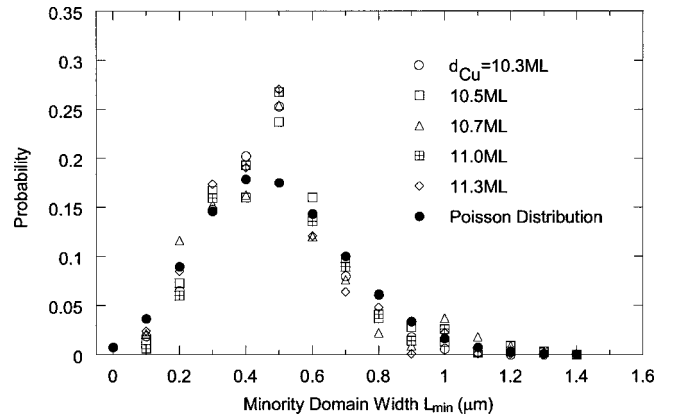


FIG. 8. Histogram of the minority stripe domain width. The average width remains unchanged despite the dramatic change of the perpendicular magnetization (M_{\perp}).

the difference of the white and dark areas of the PEEM images (Fig. 9). The results clearly show that the average minority domain size remains unchanged within the statistical range despite the significant change of the perpendicular magnetization (M_{\perp} changes from $+0.75$ to -0.73). The size distribution of the minority domain width was fit with Poisson distribution (solid dots in Fig. 8) which yields an averaged domain width of $0.49 \mu\text{m}$. The finite width of the distribution may reflect the inherent spatial fluctuations of the stripe domains.⁷

Figure 9 also gives information on the saturation magnetic field at which the stripe domains are swept out. For $d_{\text{Fe}} = 4.7$ ML, the remanence changes between -1 and $+1$ due to the oscillatory interlayer coupling, and the boundary between AFC and FC is virtually zero. For $d_{\text{Fe}} = 5.4$ ML, the formation of stripe domains obviously broadens the boundary between the AFC and FC. From the broadened range and Fig. 3, we can obtain the field needed to sweep out the stripe domains. The oscillatory coupling varies as $J = (J_0/d_{\text{Cu}}^2)\sin(2\pi d_{\text{Cu}}/\Lambda - \Phi)$ with $\Lambda = 5.8$ ML being the oscillation periodicity and Φ being a phase factor.¹⁸ For a given AFC peak, the saturation field H_S in Fig. 3 satisfies

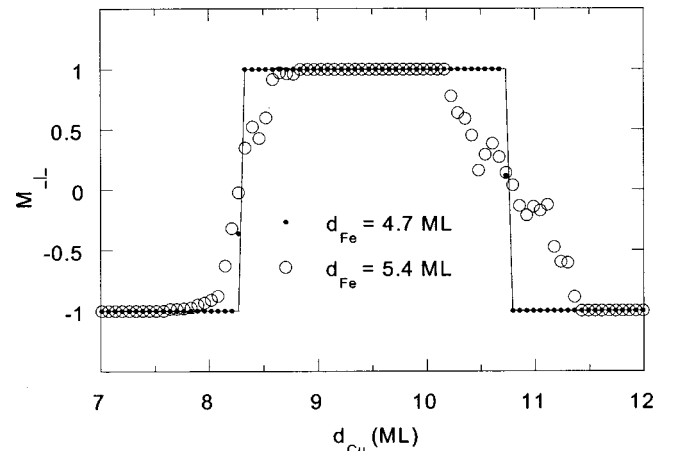


FIG. 9. Perpendicular magnetic remanence (M_{\perp}) obtained from PEEM images versus Cu thickness at $d_{\text{Fe}} = 4.7$ and 5.4 ML.

$$M_{\text{Fe}}d_{\text{Fe}}H_S = J_0M_{\text{Ni}}M_{\text{Fe}}/d_{\text{Cu}}^2. \quad (1)$$

Near the zero coupling point adjacent to that AFC peak, the coupling strength is $J \approx (J_0/d_{\text{Cu}}^2) \cdot (2\pi\delta d_{\text{Cu}}/\Lambda)$ where δd_{Cu} is the difference of the Cu thickness from the zero coupling position. Thus the virtual magnetic field satisfies

$$M_{\text{Fe}}d_{\text{Fe}}H_V = JM_{\text{Ni}}M_{\text{Fe}} \approx (J_0M_{\text{Ni}}M_{\text{Fe}}/d_{\text{Cu}}^2)2\pi\delta d_{\text{Cu}}/\Lambda. \quad (2)$$

Equation's (1) and (2) give the virtual magnetic field of $H_V \approx 2\pi H_S \delta d_{\text{Cu}}/\Lambda$. By taking the values of $H_S = 400$ Oe for the second AFC peaks at ($d_{\text{Cu}} = 12.5$ ML) and the magnetic remanence in Fig. 9, we constructed the M vs H_V curve near the two zero coupling points ($d_{\text{Cu}} = 8.4$ ML and $d_{\text{Cu}} = 10.7$ ML). The result (Fig. 10) shows that the field needed to sweep out the stripe domains is ~ 300 Oe. This value is two orders of magnitude higher than the theoretical value of ~ 0.3 Oe, which is derived from the energy difference between single domain and stripe domain phases. The apparent discrepancy may come from two sources. First, interfacial roughness and defects tend to pin domain walls and increase the saturation magnetic field.¹⁹ Berger and Hopster found that the activation energy varies from sample to sample, indicating the importance of defects.¹³ Allenspach and Bischof also noticed that the stripe domains seem to always nucleate from defects.⁵ Second, higher-order magnetic anisotropy should play a role in the SRT, where the effective uniaxial anisotropy approaches zero. The effect of quadratic anisotropy has been studied for the SRT in a single domain picture^{16,20} but not for the stripe domain phase. The above two effects should be considered in future theoretical studies.

In summary, we showed that magnetic remanence of an

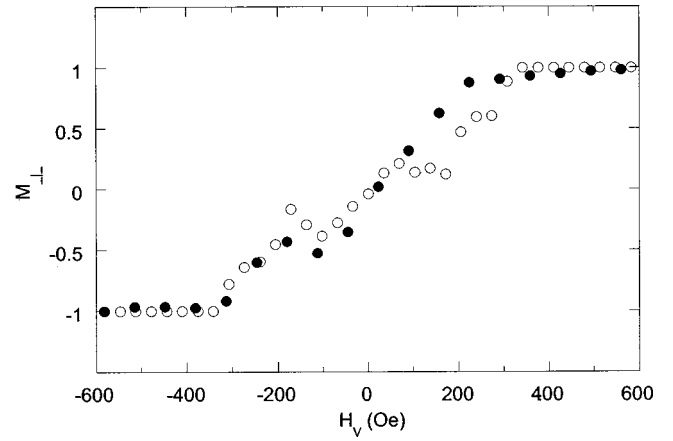


FIG. 10. Perpendicular magnetization (M_{\perp}) versus the virtual magnetic field (H_V) around the two zero coupling regions at $d_{\text{Cu}} = 8.4$ ML (filled circles) and $d_{\text{Cu}} = 10.7$ ML (open circles).

Fe film within the SRT pseudogap oscillates with the Fe-Ni interlayer coupling in the Fe/Cu/Ni/Cu(001) system. This result demonstrates the equivalence of the interlayer coupling and a virtual magnetic field. By investigating the properties of the stripe domains within the virtual magnetic field using PEEM, we showed that a perpendicular magnetic field increases the average size of the majority domains but leaves the average minority domain size unchanged.

We are pleased to acknowledge N. V. Smith for his encouragement in the pursuit of this work at the Advanced Light Source. This work was supported in part by the DOE BES-MS under Contract No. DE-AC03-76SF00098 (at LBNL) and NSF DMR-0110034.

*Permanent address: Institut für Experimentaphysik, Freie Universität Berlin, Arnimallee 14, D-14195 Berlin-Dahlem, Germany.

¹M. D. Mermin and H. Wagner, Phys. Rev. Lett. **17**, 1133 (1966).

²M. Bander and D. L. Mills, Phys. Rev. B **38**, 12 015 (1988).

³D. P. Pappas, K.-P. Kämper, and H. Hopster, Phys. Rev. Lett. **64**, 3179 (1990).

⁴Z. Q. Qiu, J. Pearson, and S. D. Bader, Phys. Rev. Lett. **70**, 1006 (1993).

⁵R. Allenspach and A. Bischof, Phys. Rev. Lett. **69**, 3385 (1992).

⁶Y. Yafet and E. M. Gyorgy, Phys. Rev. B **38**, 9145 (1988).

⁷A. Kashuba and V. L. Pokrovsky, Phys. Rev. Lett. **70**, 3155 (1993); Phys. Rev. B **48**, 10 335 (1993).

⁸Ar. Abanov, V. Kalatsky, V. L. Pokrovsky, and W. M. Saslow, Phys. Rev. B **51**, 1023 (1995).

⁹S. T. Chui, Phys. Rev. Lett. **74**, 3896 (1995).

¹⁰I. Booth, A. B. MacIsaac, J. P. Whitehead, and K. De'Bell, Phys. Rev. Lett. **75**, 950 (1995); A. B. MacIsaac, K. De'Bell, and J. P. Whitehead, *ibid.* **80**, 616 (1998).

¹¹E. Y. Vedmedenko, H. P. Oepen, A. Ghazali, J.-C. S. Levy, and J. Kirschner, Phys. Rev. Lett. **84**, 5884 (2000).

¹²A. Berger and H. Hopster, Phys. Rev. Lett. **76**, 519 (1996).

¹³R. K. Kawakami, M. O. Bowen, Hyuk J. Choi, E. J. Escorcia-Aparicio, and Z. Q. Qiu, Phys. Rev. B **58**, R5924 (1998).

¹⁴F. Nolting, A. Scholl, J. Stöhr, J. W. Seo, J. Fompeyrine, H. Siegart, J.-P. Loquet, S. Anders, J. Lüning, E. E. Fullerton, M. F. Toney, M. R. Scheinfein, and H. A. Padmore, Nature (London) **405**, 767 (2000).

¹⁵B. Schulz and K. Baberschke, Phys. Rev. B **50**, 13 467 (1994).

¹⁶K. Ha, M. Ciria, R. C. O'Handley, P. W. Stephens, and S. Pagola, Phys. Rev. B **60**, 13 780 (1999).

¹⁷H. J. Choi, E. Rotenberg, R. K. Kawakami, U. Bovensiepen, J. H. Wolfe, N. V. Smith, and Z. Q. Qiu, Phys. Rev. B **62**, 6561 (2000).

¹⁸Z. Q. Qiu, J. Pearson, and S. D. Bader, Phys. Rev. B **46**, 8659 (1992).

¹⁹D. Sander, R. Skomski, C. Schmidhals, A. Enders, and J. Kirschner, Phys. Rev. Lett. **77**, 2566 (1996).

²⁰Y. T. Millev, H. P. Oepen, and J. Kirschner, Phys. Rev. B **57**, 5837 (1998); **57**, 5848 (1998).